# CHAPTER IV

RESULT AND DISCUSSION

4.1 Study of Chemical Structure of Starch-g-Polyacrylamide and The Basic Mechanism for Graft Copolymerization

The chemical structure of graft copolymer was investigated using a FT-IR spectrophotometer. The spectrum is shown in Figure 4.1 and interpretation of the peak characteristics in given in Table 4.1. The peaks of functional groups of starch and polyacrylamide are overlapped mutually around at 3800-3000, 2923 and 1405 cm^{-1} ,indicating that mutual formation of graft copolymer and homopolymer of acrylamide are possible.

The overall reaction mechanism for the graft copolymerization via the foamed polymerization process may be proposed as follows :
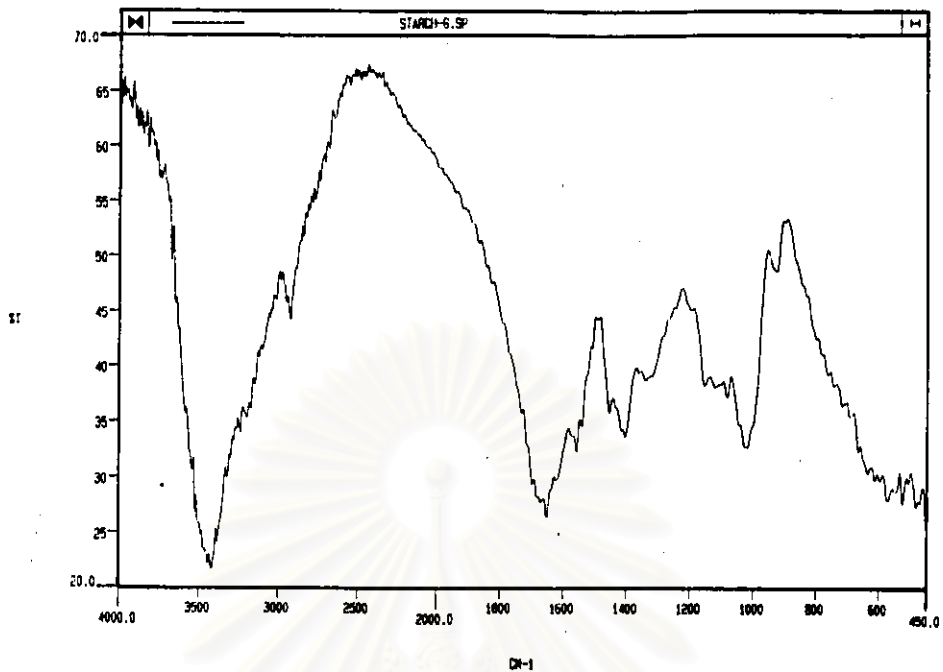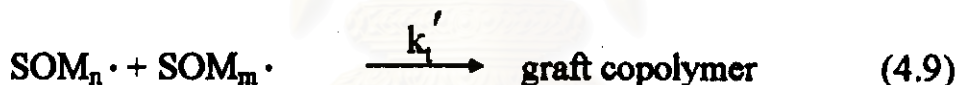
Radical formation

$$S_2O_8^{2-} \longrightarrow 2SO_4^{-\bullet} \qquad (4.1)$$

$$SO_4^{-\bullet} + H_2O \longrightarrow HSO_4^- + {}^\bullet OH \qquad (4.2)$$
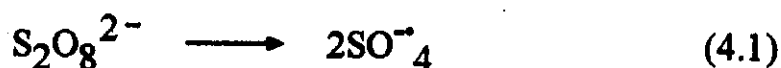
Fig. 4.1 IR spectrum of starch-g-polyacrylamide .

TABLE 4.1

Peak Assignments of IR Spectrum
of the Starch-g-Polyacrylamide .

Wave number (cm^{-1})	Assignment
3800-3000	O-H stretching
3417	N-H stretching
2923	aliphatic C-H stretching
1652	C = O stretching of amide group
1405	C-H asymmetric bending for methylene group
1019	O-H of out of plane bending

Mechanism

$$R \cdot + M \xrightarrow{k_i} RM \cdot \qquad (4.3)$$

$$RM \cdot + M \xrightarrow{k_p} RMM \cdot \qquad (4.4)$$

$$RM_{n-1} \cdot + M \xrightarrow{k_p} RM_n \cdot \qquad (4.5)$$

$$SOH + RM_n \cdot \xrightarrow{k_i'} SO \cdot + homopolymer \qquad (4.6)$$

$$SO \cdot + M \xrightarrow{k_p'} SOM \cdot \qquad (4.7)$$

$$SOM \cdot + nM \xrightarrow{k_p'} SOM_n \cdot \qquad (4.8)$$

$$SOM_n \cdot + SOM_m \cdot \xrightarrow{k_t'} graft\ copolymer \qquad (4.9)$$

where $R \cdot$ =   primary radical, $SO^{-\!\!\!\!\!*}$ or $\cdot OH$,

       M =   acrylamide monomer,

       SOH =   starch backbone.

The value of k_i' , k_p' and k_t' are initiation, propagation, and termination rate constants of the graft copolymerization, respectively. The probability of formation of homopolyacrylamide prior to the graft copolymer formation is reasonable because a large number of acrylamide molecules presented in the reaction mixture when compared to backbone. The formation of graft copolymer should be likely due to the chain transfer reaction according to Eq. (4.6). The viscosity of system before polymerization is high and therefore the gel effect is allowed to occur,

promoting the termination mode in the form of chain transfer reaction of chain radicals to the starch backbone. Further studies to confirm this postulation is required.

The isolation of graft copolymer in homogeneous system from homopolymer and reactants is complicated and not absolute. Therefore, the IR spectrum such as Fig. 4.1 may be the spectrum of graft copolymer only or the one of graft copolymer and homopolymer overlapped mutually. Further work on separation of the homopolyacrylamide from the graft copolymer are recommended to carry out.

4.2 Study of Degradation of Starch Backbone in the Presence of Alkali Foaming Agent

The products during the reaction of the carbohydrates with alkali foaming agent, Na_2CO_3 at various temperatures were carried out. The physical appearance of polymers obtained at various reaction temperature is shown in Table 4.2. Only the products from the reaction of water soluble starch with Na_2CO_3 were analysed further using a FT-IR spectrophotometer. The spectra are shown in Figures 4.2, 4.3 as well as interpretation of peak characteristics of those spectra are given in Table 4.3. DSC and TGA techniques were also used to observe transition temperature and weight loss upon heating of such the products

TABLE 4.2

Appearance of Products from
the Reaction of Carbohydrates/Na_2CO_3.

Temp. (°C)	Cassava starch	Water soluble starch	Glucose
60	White gel with dispersed Na_2CO_3	Yellow and turbid gel	Yellow solution
80	Pale brown gel	Brown gel	Brown solution
100	Brown gel	Dark brown gel	Dark brown gel

TABLE 4.3
Peak Assignments of IR Spectrum of the Water
Soluble Starch and Degradative Starch.

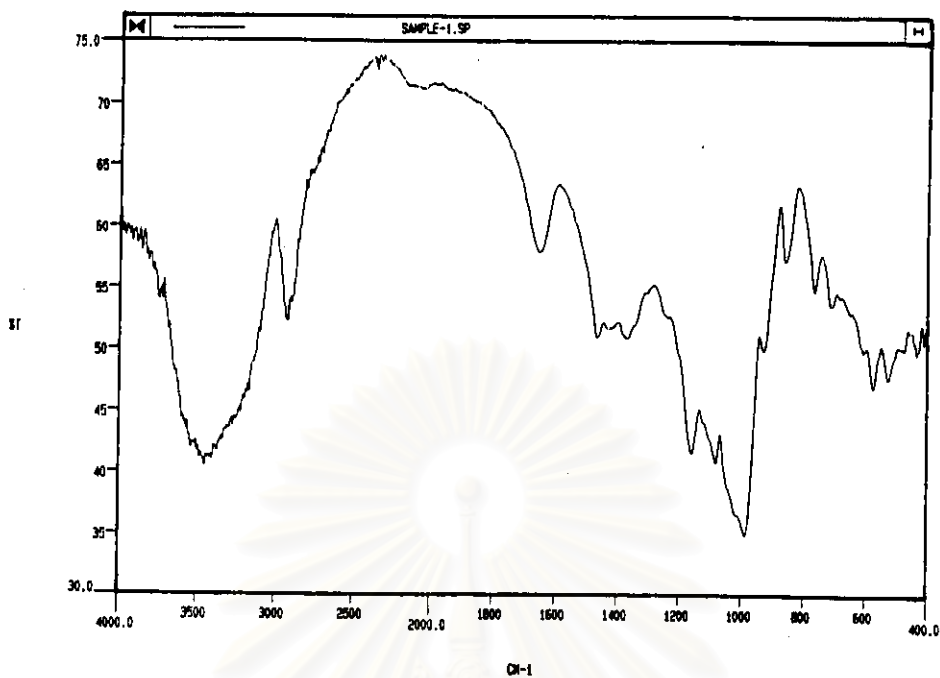| Wave number (cm^{-1})	Assignment
3800-3000	O-H stretching
2900	C-H stretching
1654	C=O stretching of aldehyde group
1160	C-O stretching of secondary alcohol
1082	C-O stretching of primary alcohol
986	O-H out of plane bending

Fig. 4.2 IR spectrum of water soluble starch .

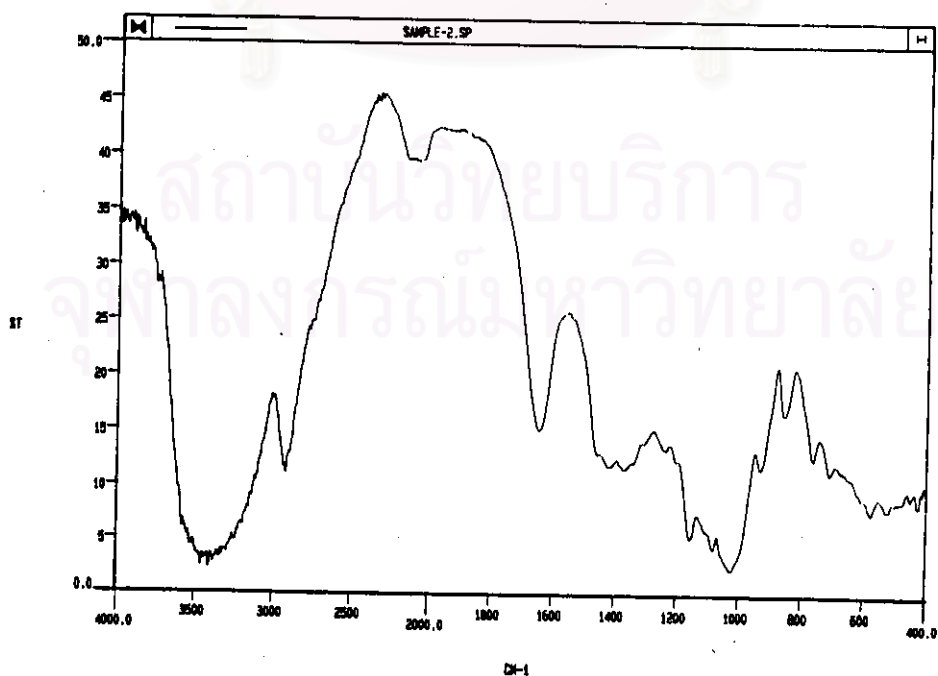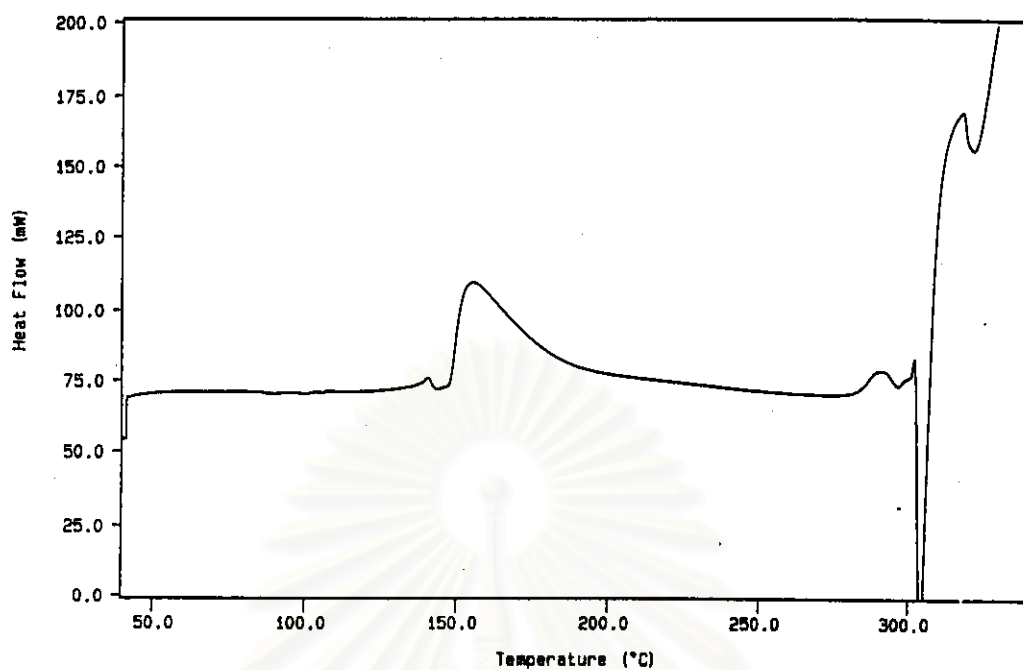

Fig. 4.3 IR spectrum of degradative starch .
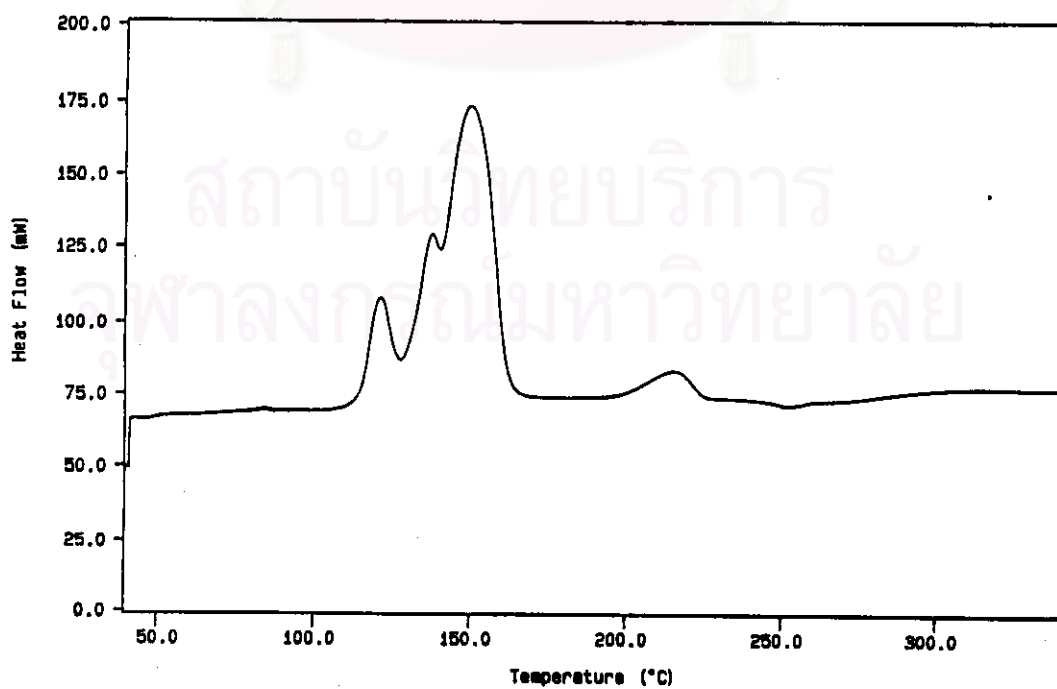
Fig. 4.4 DSC thermogram of water soluble starch.

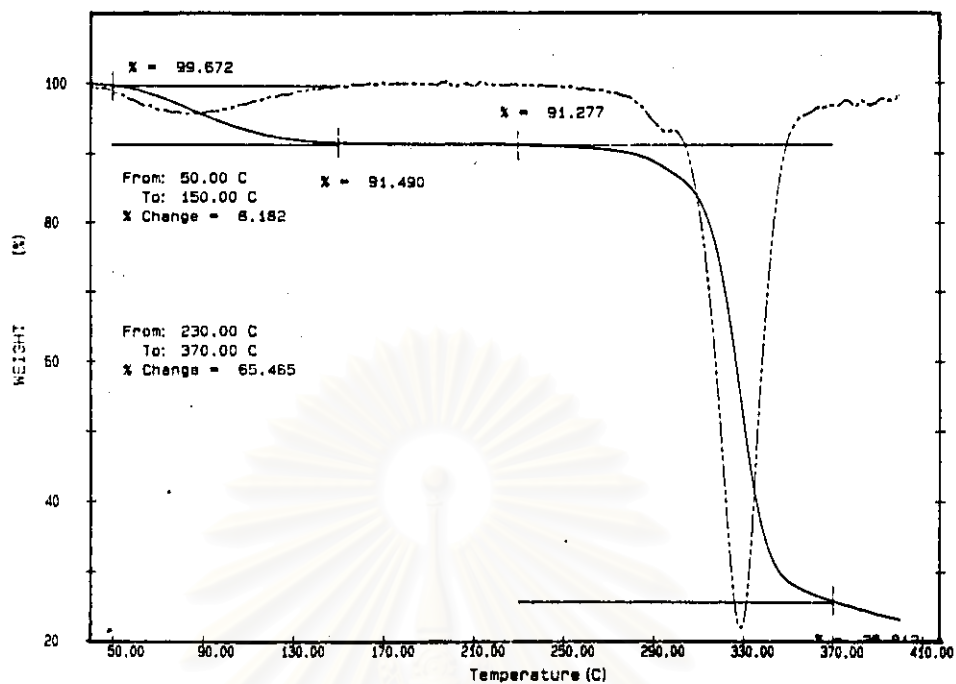
Fig. 4.5 DSC thermogram of degradative starch.

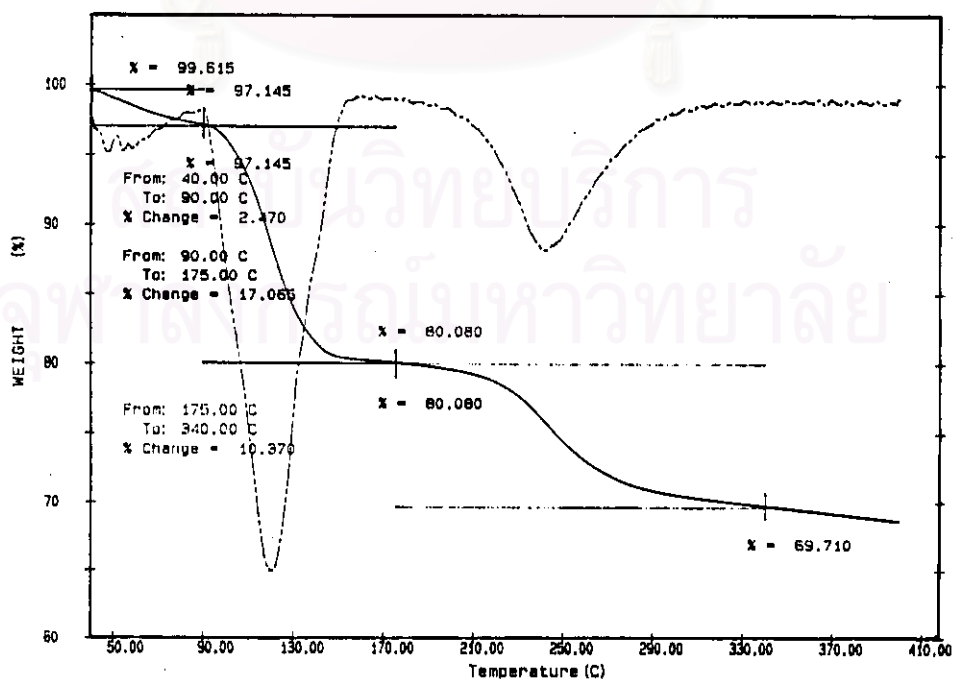Fig. 4.6 TGA thermogram of water soluble starch .

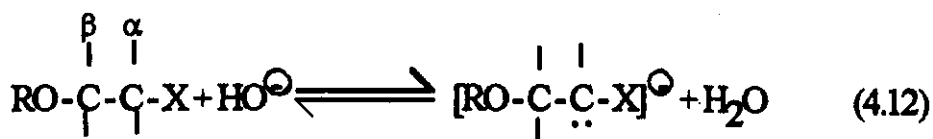Fig. 4.7 TGA thermogram of degradative starch .

Figures 4.4 and 4.5 are the DSC thermograms , while those of TGA thermograms in Figure 4.6 and 4.7.

The carbohydrate has D-glucose unit at the chain ends in its molecular structure. It often undergoes mutarotation resulting from the opening and closing of hemiacetal ring. In the open- chain, form D-glucose contains aldehyde groups as shown below.

$$(4.10)$$

$$(4.11)$$
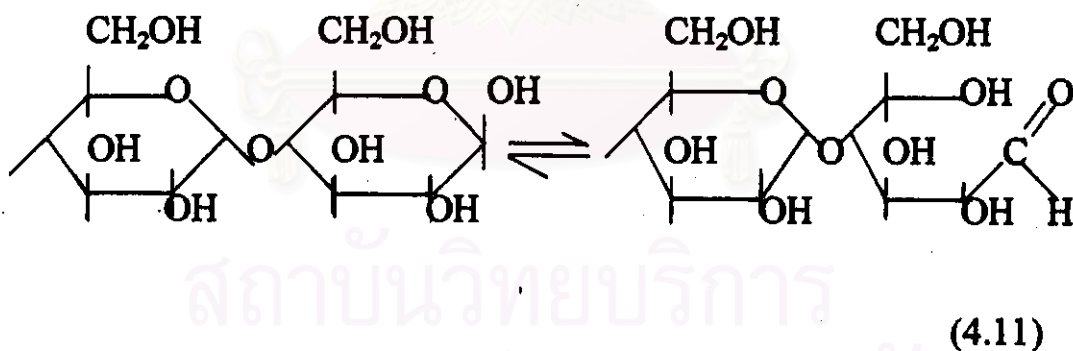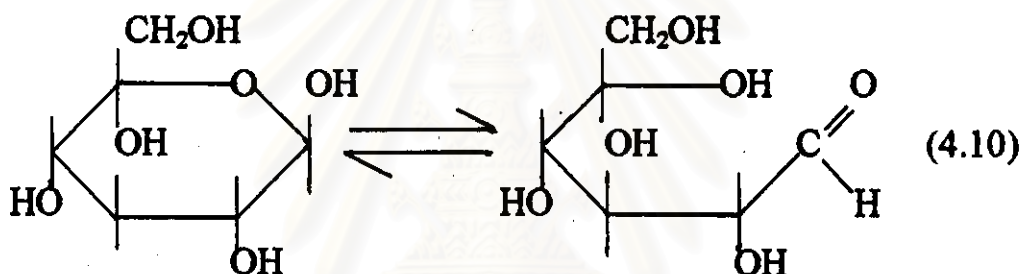
mutarotation

The presence of aldehyde group in the structure of glucose or starch can lead to oxidative degradation of molecule at the alkaline pH values. The alkali-catalysed oxidation of glucose or starch takes place by the α - proton abstraction and cleavage by β-elimination according to the chemical reactions shown below (27).

$$\text{RO-}\overset{\overset{\beta}{|}}{\underset{|}{C}}\text{-}\overset{\overset{\alpha}{|}}{\underset{|}{C}}\text{-X+HO}^{\ominus} \rightleftharpoons \text{[RO-}\overset{|}{\underset{|}{C}}\text{-}\overset{|}{\underset{..}{C}}\text{-X]}^{\ominus}\text{+H}_2\text{O} \qquad (4.12)$$

$$\text{[RO-}\overset{|}{\underset{|}{C}}\text{-}\overset{|}{\underset{..}{C}}\text{-X]}^{\ominus} \longrightarrow \text{[RO:]}^{\ominus}\text{+[}\overset{|}{\underset{|}{C}}\text{=CX]} \qquad (4.13)$$

$$\text{[RO:]}^{\ominus}\text{+H}_2\text{O} \longrightarrow \text{ROH + HO}^{\ominus} \qquad (4.14)$$

where   R   =   H, anhydroglucose units attached

X   =   aldehyde group

The results in Table 4.2 show the products from the alkali-catalysed oxidative degradation of carbohydrates by Na_2CO_3 alkali foaming agent, which should also occur in the foamed polymerization to synthesize of starch-g-polyacrylamide due to Na_2CO_3 dissolved in aqueous starch gel at 80°C of the preparation stage. The oxidative degradation is more serious when higher temperature was employed. For the higher concentration of aldehyde group of starch ,the more serious oxidative degradation occurred. Therefore a dark brown gel was obtained .

Therefore, in the equal concentration, the system in the presence of glucose contains relatively a great number of aldehyde groups which will undergo alkali-catalysed oxidative degradation seriously.

In the case of starch used as the backbone in the graft copolymerization, the alkali-catalysed oxidative degradation is the cleavage of glycosidic linkage, leading to chain scission and lowering in molecular weight and chain length of the backbone. Figures 4.2 and 4.3 ;Table 4.3 shows that most of functional groups have no change, indicating that

oxidative degradation leads to chain scission rather than degradation to new products.

The results from Figure 4.4, 4.5, 4.6 and 4.7 implies that the splitting of peaks of decomposition in DSC and TGA thermograms in the same pattern results from the decomposition of the same type of structural region but different sizes of ones.

4.3 Study of Chemical Structure of Polyacrylamide and the Basic Mechanism for Polymerization of Acrylamide

In the synthesis of starch-g-polyacrylamide using the foamed polymerization described in Section 4.1, the polymeric product preferably consists of starch-graft copolymer and homopolymer according to the proposed mechanism. The separation of two products can not be made completely. From Section 4.2 the water soluble starch, standard backbone with known molecular weight and molecular weight distribution, experienced the alkali-catalysed oxidative degradation, which leads to chain scission and the degradative starch appearing as yellow to brown color. These two events affect to the first step of the kinetic analyses of the foamed polymerization in that it is rather complicated and ambiguous.

The synthesis of homopolyacrylamide using the foamed system was then investigated whether it could be synthesized. Upon successful,

the kinetic analysis of the foamed polymerization of acrylamide would be studied because of its simplification in comparison to the more complicated kinetics of the foamed polymerization of the starch-g-polyacrylamide.

The chemical structure of polyacrylamide the synthesized using method described in Section 3.33 was investigated by a FT-IR spectrophotometer. The spectrum is displayed in Figure 4.8 and a interpretation in Table 4.4
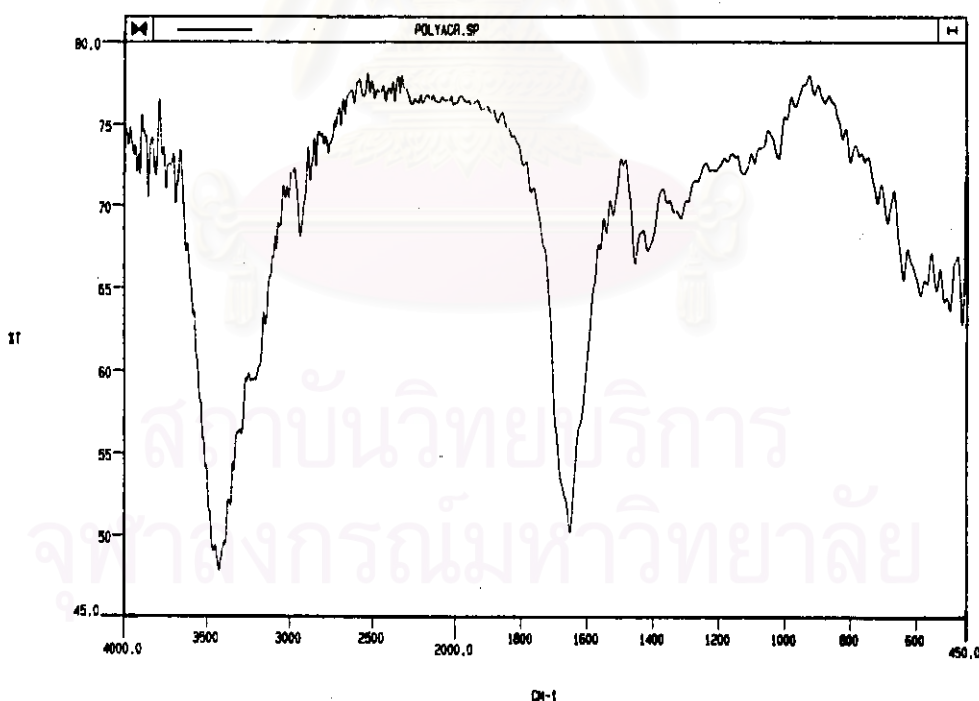

Fig. 4.8 IR spectrum of polyacrylamide .

TABLE 4.4

Peak Assignments of IR spectrum
of Polyacrylamide.

Wave number (cm^{-1})	Assignment
3427	N-H stretching
2938	aliphatic C-H stretching
1652	C = O stretching of the amide groups
1455, 1417	C-H asymmetric bending for methylene groups
1316	C-N aliphatic stretching

The sharp and distinct peaks correspondent to acrylamide functional groups are clearly obtained. The reaction mechanism of the foamed polymerization of acrylamide is proposed and shown below.

Radical formation

$$S_2O_8^{2-} \xrightarrow{k_d} 2SO_4^{-\cdot} \qquad (4.15)$$

$$SO_4^{-\cdot} + H_2O \xrightarrow{k_H} HSO_4^- + {}^\cdot OH \qquad (4.16)$$

Initiation

$$SO_4^{-\cdot} + M \xrightarrow{k_{i1}} R_1^\cdot \qquad (4.17)$$

$$^\cdot OH + M \xrightarrow{k_{i2}} R_1^\cdot \qquad (4.18)$$

Propagation

$$R_1^\bullet + M \xrightarrow{k_p} R_2^\bullet \qquad (4.19)$$

$$R_r^\bullet + M \xrightarrow{k_p} R_{r+1}^\bullet \qquad (4.20)$$

Chain transfer

$$R_r^\bullet + X \xrightarrow{k_{fx}} P_r + X^\bullet \qquad (4.21)$$

Termination

$$R_r^\bullet + R_s^\bullet \xrightarrow{k_{td}} P_r + P_s \qquad (4.22)$$

From Eq.4.2 Kolthoff, I.M. and Miller, I.K. (28) showed that sulfate radicals can react with water to produce hydroxy radicals which can perform as an initiator, k_H is the rate constant for the reaction between sulfate radial and water, k_{i1}, k_{i2} are the rate constants for the initiation reaction by $SO_4^{\bullet-}$ and $^\bullet OH$ radicals, respectively.

M   is acrylamide monomer,

$R_1^\bullet$ is the primary radical,

$R_r^\bullet$ is the propagating radical with r acrylamide molecules,

R_p is the propagation rate constant,

X   may be monomer, initiator, solvent, polymer and specially propylene glycol used in these studies as chain transfer agent,

k_{fx} is the rate constant for the chain transfer reaction.

With acrylamide termination is exclusively dominated by disproportionation reaction (29), (30), (31) ,where k_{td} is the rate constant for the termination by disproportionation. P_r, P_s are dead polymer containing r and s monomer units, respectively.

4.4 Kinetic Analysis of Isothermal Foamed Polymerization of Acrylamide

The system of polymerization in Section 4.3 was used for the kinetic analysis in the non-isothermal system because the temperature of system was allowed to rise exothermically. Indeed, in the kinetic analysis of a reaction, one should know firstly the kinetics of the isothermal condition is held so as to use the kinetic information to investigate the kinetics of the non-isothermal condition. In these studies, the kinetics of acrylamide polymerization in the isothermal foamed system was also firstly investigated.

The initial rate of polymerization of acrylamide was determined from the measurement of heat of reaction of the polymerization solution in DSC according to the method described in Section 3.4.1. Figures 4.9 and 4.10 show the typical DSC thermograms usually obtained from these experiments.

The heat of reaction of the solution under scanning mode, ΔH_S , is 129.600 J/g and that under that isothermal mode, ΔH_I ,is 14.056 J/g. The heat of reaction of the residual monomer in solution was also deter-

mined by DSC but no peaks of the heat of reaction appeared. (discussed in Section 4.4.1). Calculation of the monomer conversion and its percentage of conversion against time were achieved using Eq. 3.1. Figure 4.11 shows the plot of monomer conversion percentage against time.

It is clear from Figures 4.10 and 4.11 that the polymerization occured after an induction period, which was possibly due to residual impurities and insufficiently monomer purification (10). The conversion was reached to only 10.85 %. The limiting conversion is discussed subsequently in Section 4.4.1 . The initial rate of polymerization was determined to be 5.5676×10^{-4} mol/L-s
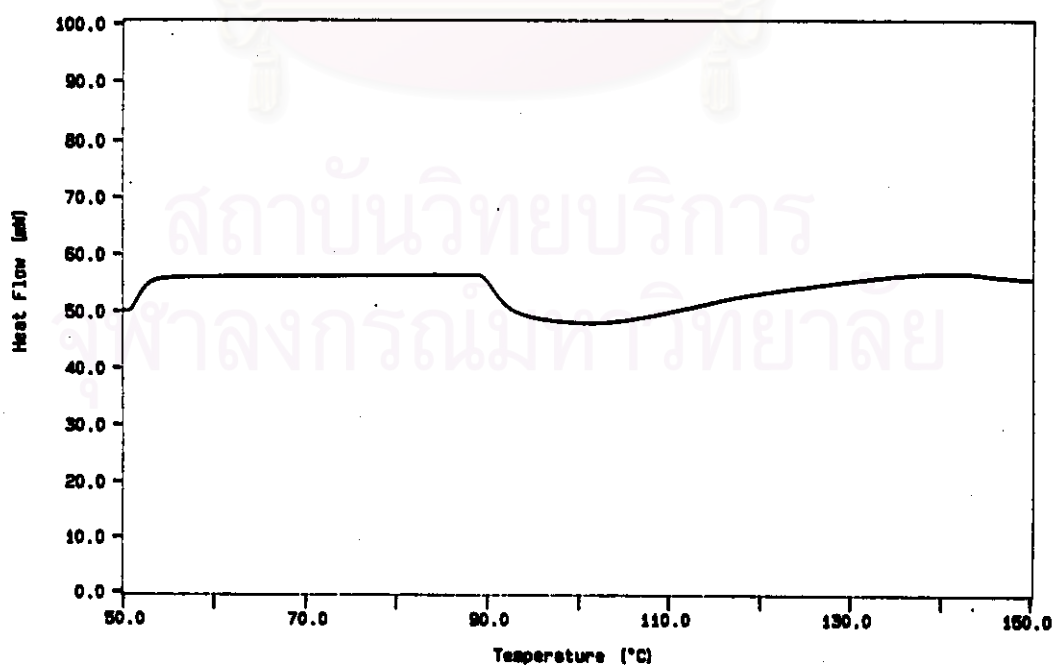
Fig. 4.9 DSC thermogram of the foamed polymerization of acrylamide ; [AM] = 2.44 mol/L , [K₂S₂O₈] =1.22 x 10⁻³ mol/L .

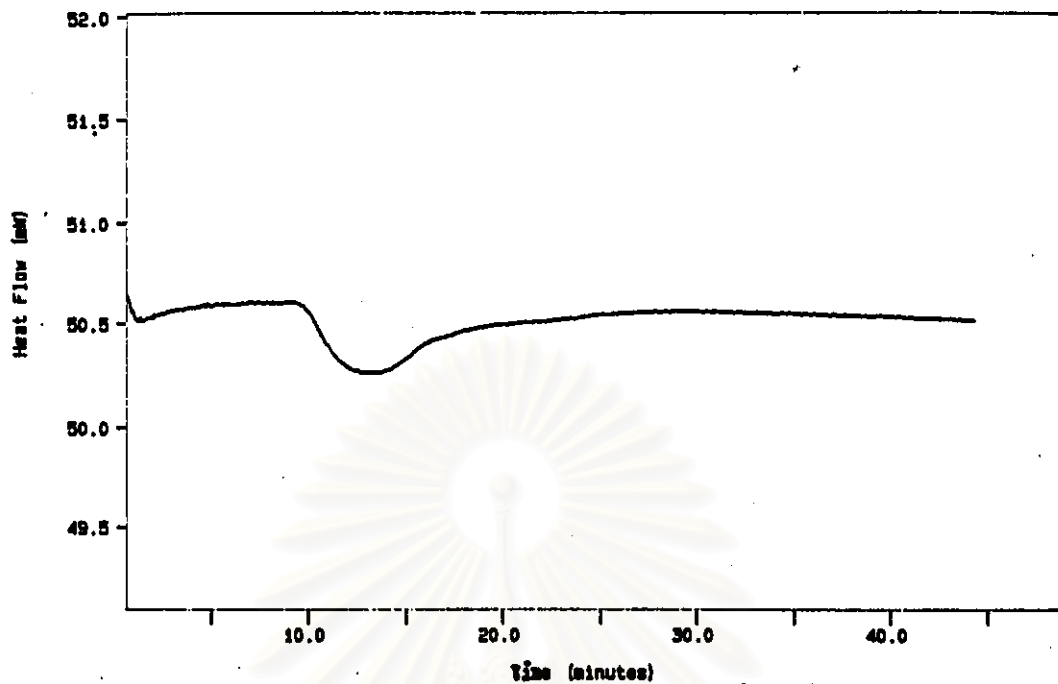Fig. 4.10 DSC thermogram of the isothermal foamed polymerization of acrylamide at 70° C ; [AM] =2.44 mol/L , [K$_2$S$_2$O$_8$] = 1.22 x 10^{-3} mol/L .
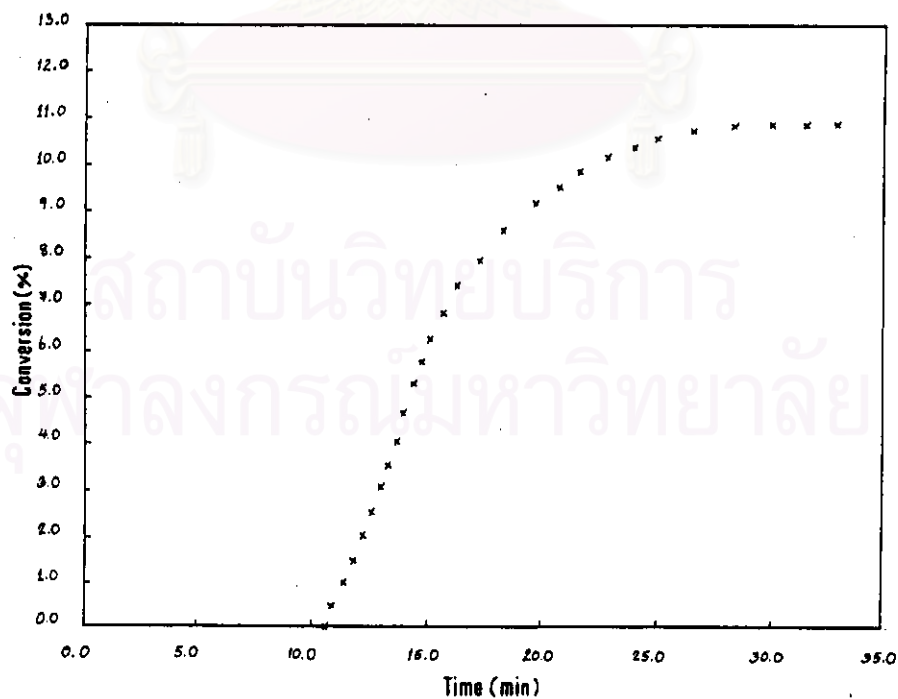

Fig. 4.11 The plot of percentage of monomer conversion versus time of acrylamide polymerization in the foamed system at 70° C ; [AM] = 2.44 mol/L ,[K$_2$S$_2$O$_8$] = 1.22 x 10^{-3} mol/L .

Based on the proposed mechanism in Section 4.3 and the steady state assumption ,the rate expression can be expressed as

$$R_p = \frac{-d[M]}{dt} = k_p \left(\frac{k_i}{k_t}\right)^{1/2} [M]\,[I]^{1/2} \qquad (2.15)$$

In practice the deviation in monomer order and initiator order are always found in many polymerization systems. Therefore for the free radical polymerization the rate is typically expressed in the form : (17)

$$R_p = \frac{-d[M]}{dt} = k_p \left(\frac{k_i}{k_t}\right)^{1/2} [M]^x\,[I]^y \qquad (4.23)$$

where $[M]$ = monomer concentration,

$[I]$ = initiator concentration,

R_P = the rate of polymerization,

x = monomer order,

y = initiator order,

and k_p, k_i and k_t are the rate constants for the propagation, the initiation and the termination, respectively.

4.4.1 Initial Rate Dependency on Monomer Concentration

The heat of polymerization of acrylamide in the foamed system under isothermal mode DSC run as well as under scanning mode were also investigated.   The percentage of monomer conversion was found to increase with increase in the concentration of monomer in the ranges of 2.44 to 3.66 mol/L (see Fig 4.12, Table 4.5 and Fig. 4.13).

No peaks of heat of polymerization of the residual monomer obtained from DSC thermogram was found.

The initial rates of polymerization were also found to increase with the increase of monomer concentration as shown in Figure 4.14.

It is obvious that on increasing the concentrations of monomer. The propagating polymer chains add more monomer units. Therefore that brings about an increase in the heat of polymerization, conversion ,and ultimately the initial rate of polymerization.
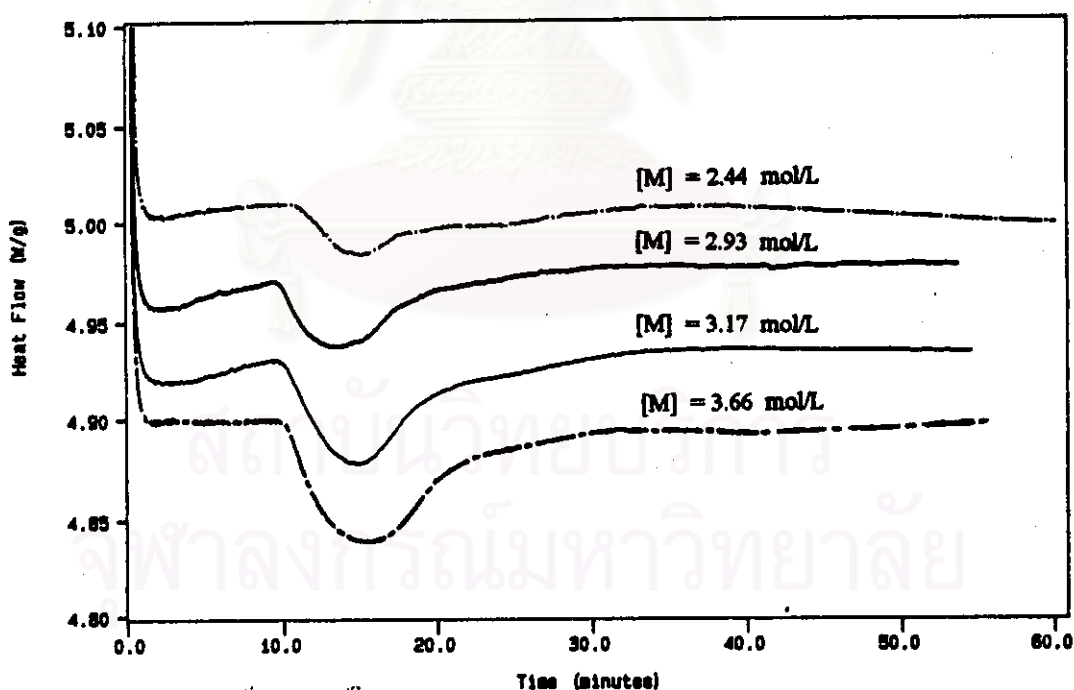

Fig.4.12 DSC thermograms of the isothermal foamed polymerization of acrylamide at $70^\circ C$; [$K_2S_2O_8$] = 1.22×10^{-3} mol/L with variation of [AM] indicated on the curves .

TABLE 4.5

Heat of Polymerization and Limiting Acrylamide Conversion

in the Foamed Polymerization of Acrylamide with

Variation of Acrylamide Concentration.

[M] (mol/L)	ΔH_S (J/g)	ΔH_I (J/g)	Limiting conversion (%)
2.44	129.600	14.056	10.85
2.93	175.613	19.885	11.32
3.17	188.564	27.475	14.57
3.66	204.440	33.133	16.21

The initial rate of polymerization was found to be proportional to the monomer concentration raised to the 1.21 power (monomer order), which is higher than the normal value of unity in rate expression based on the steady state assumption. Riggs and Rodriguez (32) reported also an unusual rate dependence for the aqueous acrylamide polymerizations initiated with potassium persulphate:

$$R_P = K \, [M]^{1.25} \, [I]^{0.5} \qquad (4.24).$$

Many investigations have confirmed a monomer dependency exceeding to the first order, which is frequently to the power 1.2 to 1.5 (33).
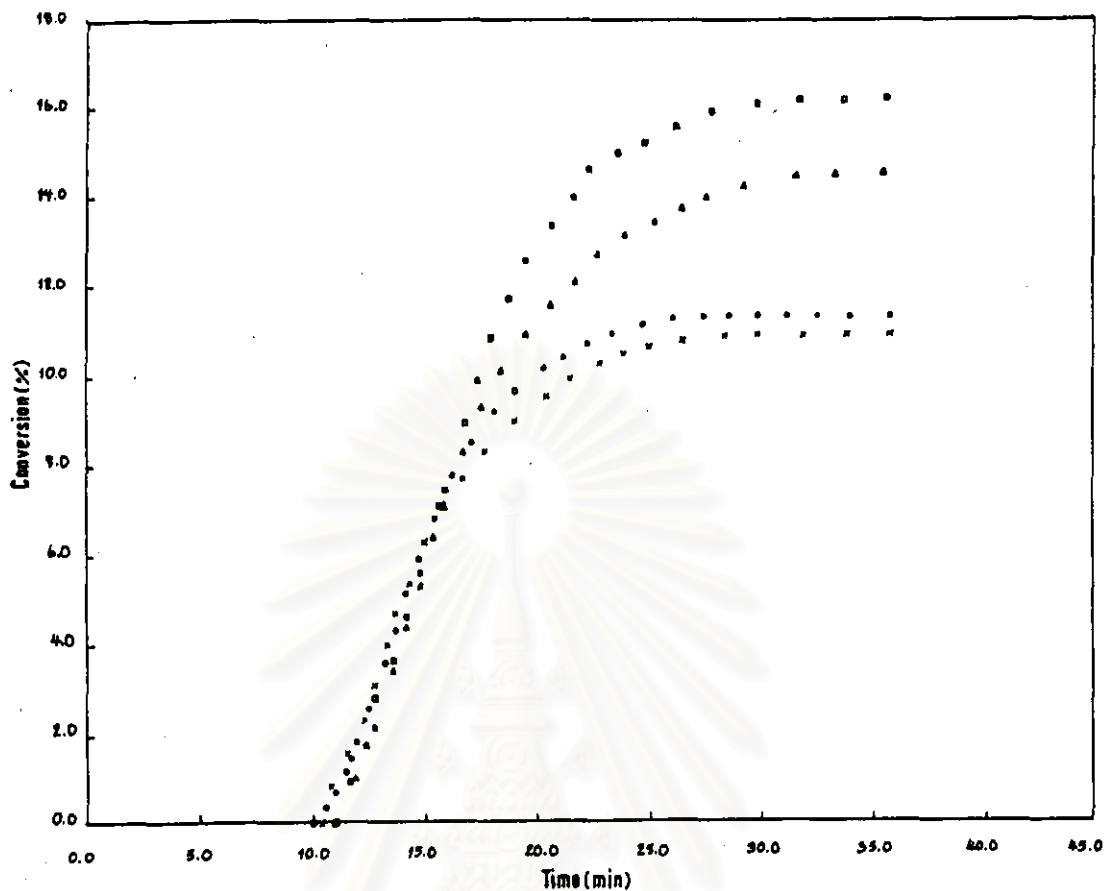
Fig.4.13 The plot of percentage of monomer conversion versus time of acrylamide polymerization in the foamed system at 70° C ; $[K_2S_2O_8]$ = 1.22 x 10^{-3} mol/L with variation of [AM] : (X) 2.44, (O) 2.93, (Δ) 3.17, ($\square$) 3.66 .
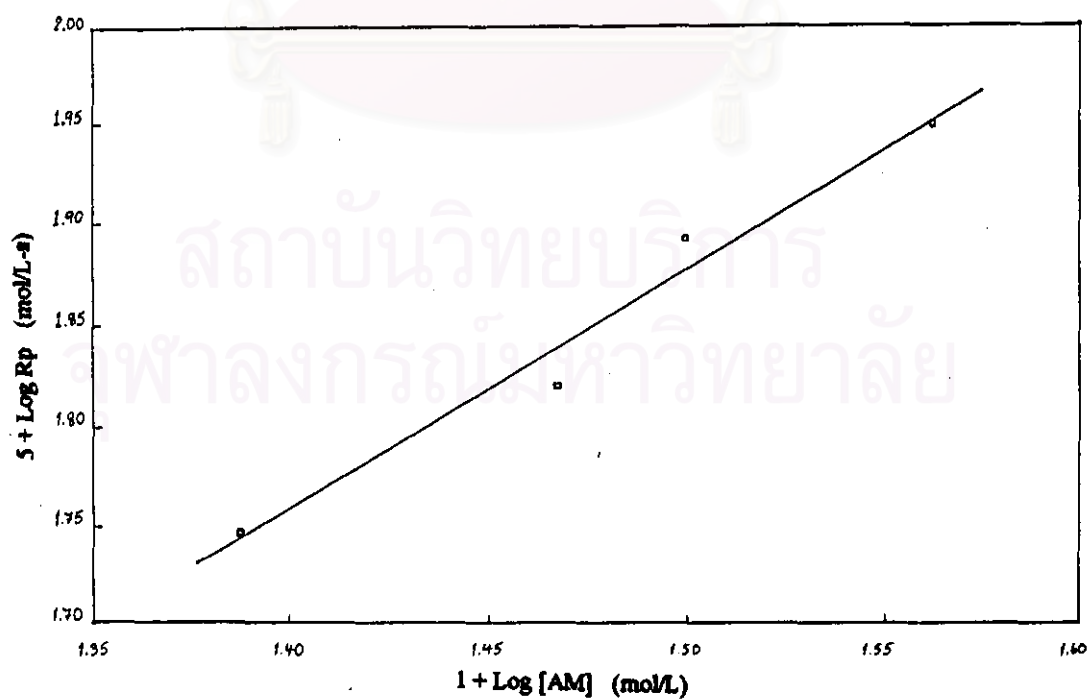

Fig. 4.14 The log - log plot of Rp vs. [AM] of acrylamide polymerization in the foamed system at 70° C ; $[K_2S_2O_8]$ = 1.22 x 10^{-3} mol/L .

Riggs and Rodriguez (34) interpreted the high rate order as evidence of monomeric influence on the rate of initiation. Hunkeler, D. (25) proposed a new mechanism to account for the high rate order with respect to monomer. It is called a "hybrid cage-complex" mechanism. It assumed that free radicals produced from the dissociation of potassium persulphate initiator are contained in a cage of solvent molecules. The existence of two cage entities were defined as : "compact cage" where the radicals were separated by less than one molecular diameter and "diffused cage" where the radicals had diffused further apart. The latter was only susceptible monomer attack. The radical pair in the cage might combine several times before diffusing out of the cage and initiating the polymerization reaction.

According to the hybrid cage-complex mechanism, the introduction of hydrogen bonding between acrylamide monomer and the free radicals from the dissociation of potassium persulphate in the diffused cage leads to monomer-initiator association process, this process leads to donor-acceptor interactions between the amide and the persulphate. The decomposition of this charge-transfer complex occurs subsequently and leads to a secondary initiation reaction, which proceeds in competition with and often in preference to the thermal bond rupture of persulphate.
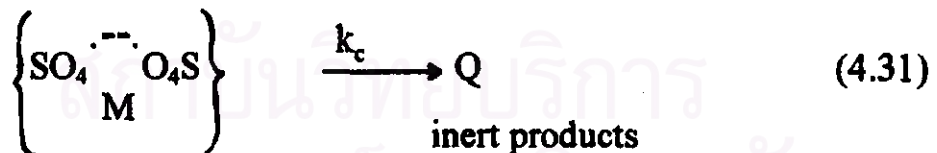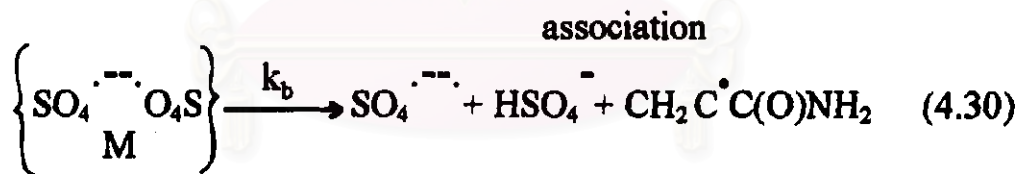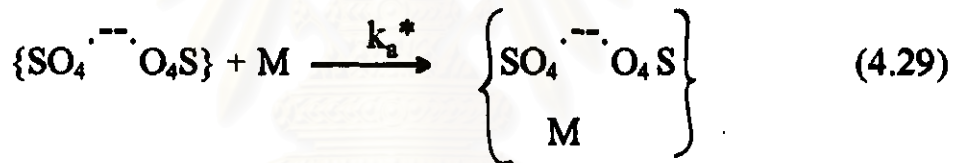
The equations representing the mechanism are shown below :

Initiator reactions (Formation of a cage hierarchy)

$$S_2O_8^{2-} \quad \underset{k_1'}{\overset{k_1}{\rightleftarrows}} \quad (SO_4^{\bullet--}O_4S) \qquad (4.25)$$

$$(SO_4^{\bullet--}O_4S) \xrightarrow{k_2} \{SO_4^{\bullet--}O_4S\} \qquad (4.26)$$

$$\{SO_4^{\bullet--}O_4S\} \xrightarrow{k_d^*} 2SO_4^{\bullet-} \qquad (4.27)$$

$$\{SO_4^{\bullet--}O_4S\} \xrightarrow{k_r} S_2O_8^{2-} \qquad (4.28)$$
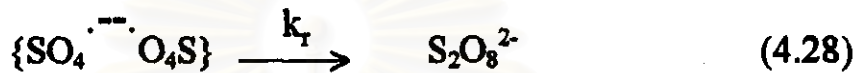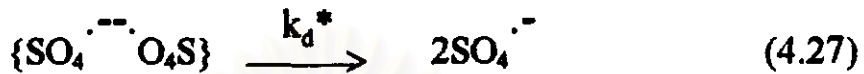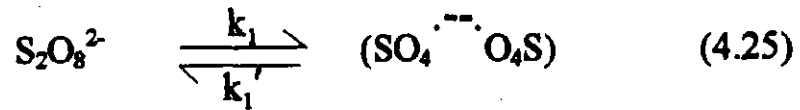
Parenthesis indicate a "compact cage" and Braces signify a "diffused cage".

<u>"Association" (swollen cage formation) and Decomposition</u>

$$\{SO_4^{\bullet--}O_4S\} + M \xrightarrow{k_a^*} \left\{ \begin{array}{c} SO_4^{\bullet--}O_4S \\ M \end{array} \right\} \qquad (4.29)$$

<div align="center">association</div>

$$\left\{ \begin{array}{c} SO_4^{\bullet--}O_4S \\ M \end{array} \right\} \xrightarrow{k_b} SO_4^{\bullet--} + HSO_4^- + CH_2C^{\bullet}C(O)NH_2 \qquad (4.30)$$

$$\left\{ \begin{array}{c} SO_4^{\bullet--}O_4S \\ M \end{array} \right\} \xrightarrow{k_c} Q \qquad (4.31)$$

<div align="center">inert products</div>

Eq. 4.30 represents the dissociation through a donor-acceptor intermediate. Eq. 4.31 represents the consumption of monomer-initiator associates through a reaction that generates non reactive products. This initiator deactivation is necessary to avoid nonunit efficiencies of the initiation.

<u>Chain Initiation</u>

$$SO_4^{\bullet-} + M \xrightarrow{k_{i1}} R_1^{\bullet} \qquad (4.32)$$

$$SO_4^{\cdot --} + H_2O \xrightarrow{k_H} HSO_4^{\cdot -} + {\cdot}OH \qquad (4.33)$$

$${\cdot}OH + M \xrightarrow{k_{i2}} R^{\cdot}_1 \qquad (4.34)$$
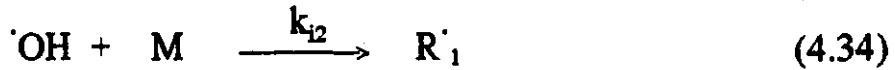
Propagation through termination is similar to the equations shown in Section 4.3. This mechanism involves the monomer-enhanced decomposi-tion of potassium persulfate distinctly. The hybrid mecha-nism is further characterized by two com-peting initiation process : thermal bond rupture and monomer-enhanced decomposition. These yield the following rate equations.

Thermal decomposition dominates

$$R_p = k_p \ [M] \left(\frac{2fk_d[I]}{k_{td}} \right)^{1/2} \qquad (4.35).$$

Monomer - enhanced decomposition dominates

$$R_p = k_p \ [M]^{3/2} \left(\frac{2f_c k_a[I]}{k_{td}} \right)^{1/2} \qquad (4.36).$$

The overall polymerization rate order with respect to monomer concentration is therefore governed by the relative rate constants of thermal decomposition (k_d) and association (k_a) and their respective initiation efficiency (f, f_c). Therefore, the monomer order in the present research work implies that two types of initiations can occur in the polymerization of acrylamide in the foamed system. In addition the hybrid mechamism can be used to elucidate the limiting conversion and peak of heat of polymerization of residual monomer disappeared.

Incomplete monomer consumption is generally attributed to either a depletion of the initiator or isolation of the macroradicals (gel

effect and glass effect). These phenomena can be distinguished by raising the temperature after the limiting conversion is reached. If residual initiator is present but is physically hindered from reaching the acrylamide monomer, increasing the thermal energy to the system will increase the diffusion of small molecules and increase the rate.

In the DSC run for determining the heat of polymerization of residual monomer but no peaks appeared in spite of no gel effect in these studies. This indicates the initiator concentration has previously been exhausted from the reaction. The conversion was limited and the limiting conversion is the evidence of a second initiator decomposition reaction noticeably.

4.4.2 Initial Rate Dependency on Initiator Concentration

The heat of polymerization of acrylamide, the percentage of conversion and the initial rate of polymerization of acrylamide in the foamed system increased when the initiator concentration increases ,which is in the studied ranges from 0.0012 to 0.0061 mol/L . The results of the three events are shown in Fig. 4.15 and Table 4.6; Fig. 4.16 ; Fig.4.17 ,respectively.

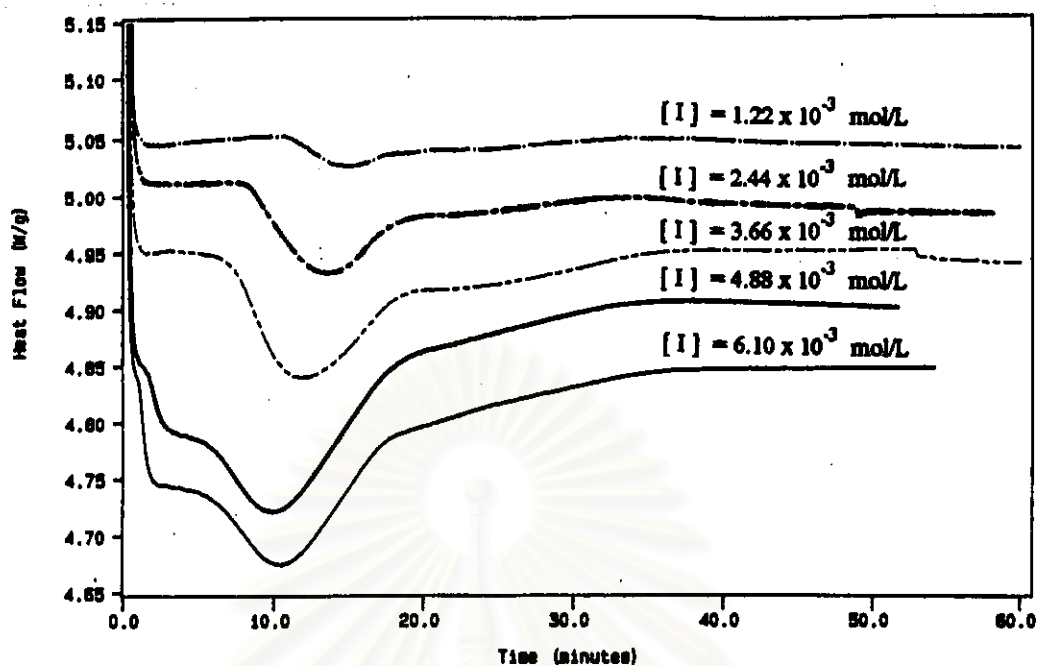No peaks of heat of polymerization of the residual monomer determined by DSC was observed.

Fig. 4.15 DSC thermograms of the isothermal foamed polymerization of acrylamide at 70°C ; [AM] = 2.44 mol/L with variation of [K₂S₂O₈] indicated on the curves .

TABLE 4.6

Heat of Polymerization and Limiting Acrylamide Conversion in the

Foamed Polymerization of Acrylamide with Variation of

Potassium Persulphate Concentration.

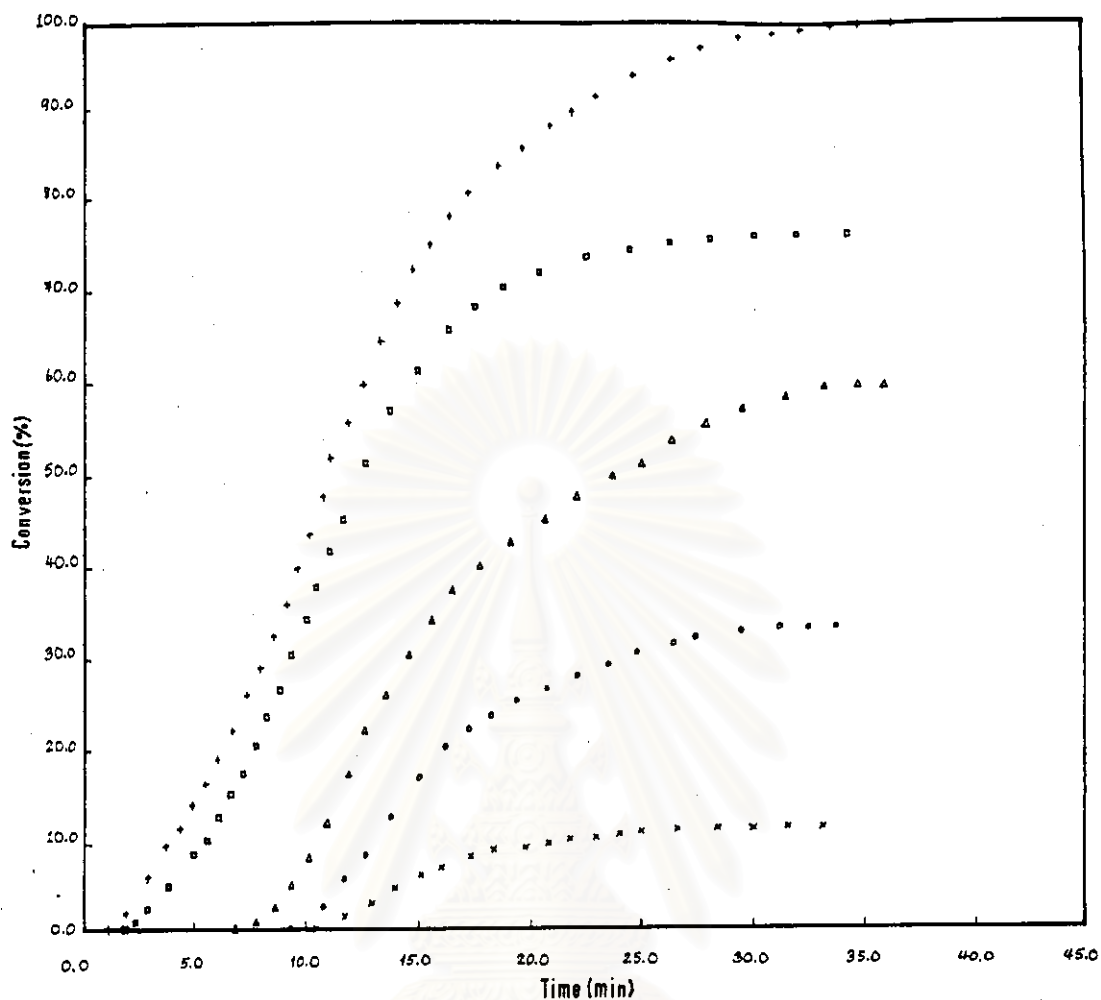| [I] (mol/Lx10³)	ΔH$_S$ (J/g)	ΔH$_I$ (J/g)	Limiting conversion (%)
1.22	129.600	14.056	10.85
2.44	129.620	43.063	33.22
3.66	129.673	77.739	59.95
4.88	129.685	99.012	76.35
6.40	131.710	131.616	99.93

Fig. 4.16 The plot of percentage of monomer conversion versus time of acrylamide polymerization in the foamed system at 70° C ; [AM] = 2.44 mol/L with variation of $[K_2S_2O_8]$: (X) 1.22, (O) 2.44, (Δ) 3.66, ($\square$) 4.88, (+) 6.10 x 10^{-3} mol/L .

On increasing the concentration of initiator, the number of initiating species (free radicals $R^\bullet$) increases, leading to the increase in the growing chain population, which, inturn, increases the rate of polymerization, the percentage of monomer conversion and the heat of polymerization.

From the log-log plot shown in Fig.4.17, the dependence of polymerizationrate on initiator concentration was found to be proportional to initiator concentration raised to the 0.5 power (initiator order).
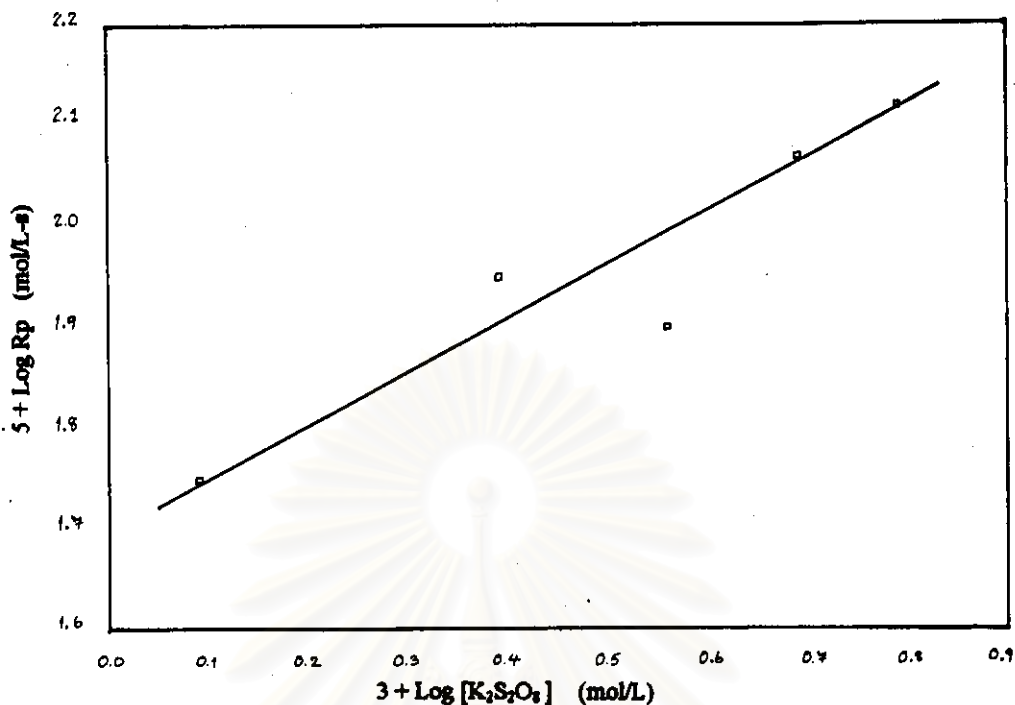
Fig. 4.17 The log - log plot of Rp vs. $[K_2S_2O_8]$ of acrylamide polymerization in the foamed system at 70°C ; [AM] = 2.44 mol/L .

The order with respect to initiator, found to be one-half indicates that the termination occurs predominantly through a mutual combination of polymer chain radicals (35).

The results from Figs.4.15 and 4.16 show that the more the iniator concentration; the shorter the induction period achieves. The reason is that the more initiating species consume the impurities acting as inhibitor faster, reducing the induction period. At the end of this period polymerization proceeds at the same rate as in the absence of initiator.

In addition, the results from Figs.4.15 and 4.16 show the gel effect (Sec.tion 2.3.3) when the initiator concentrations are above 3.66 x 10^{-3} mol/L. The gel effect in the system most likely results from two causes. Firstly, the high free radicals in the system lead to the faster

initial rate of polymerization. The viscosity of system increases fast, leading to the occurrence of the get effect. Lastly, the foamed system consists of the mixture of a large number of gas bubbles and gel-like particles promoting the gel effect significantly (Section 2.2).

The gel effect is not found in aqueous solution polymerization system in the presence of the same range of acrylamide and potassium persulphate concentrations when the results is compared to those in the foamed system studied. From the results of Section 4.4.1, it is apparent that no gel effect is found in the system and the reaction behavior is similar to the one in aqueous solution polymerization system. The only difference is that one can produce the porous-gel polymeric product. The low free radicals in the system are the reason why no gel effect was found. Therefore the gel effect in the foamed polymerization of acrylamide under the isothermal condition is a new distinct observation.

The gel effect in the system also yields high limiting conversion. When the initiator concentration increases in the range without gel effect appearance ,the limiting conversion is influenced by the hybrid mechanism as mentioned earlier in Section 4.4.1. When the increase in initiator concentration is reached to a given value that the gel effect occurs, the limiting conversion is affected by the hybrid-mechanism and the gel effect.

Refering to the equation of the rate expression (4.23), one can propose the rate expression of acrylamide polymerization in the foamed

system under the isothermal condition (initial polymerization rate)   by using the results above in the form of

$$R_p = K [M]^{1.21} [I]^{0.5} \qquad (4.37)$$

where K is the overall rate constants of polymerization

.   The average over all rate constant, K at 70°C is determined using the above equation to be 5.45x10^{-3} L/mol-s within the tolerance of 5%.

4.4.3 The Effect of Polymerization Temperature on Initial Rate

When the temperature of the reaction system was increased in the   ranges of 70-90°C ,the heat of polymerization, percentage of conversion and initial rate of polymerization of acrylamide in the foamed system increased (Fig.4.18, Table 4.7, Fig 4.19 and Fig 4.20). No peaks of heat of polymerization of residual monomer detected by DSC was found. Those values increased due to the rise in the rate of radical generation and propagation steps.

The Arrhenius plot allows to determine the overall activation   energy to be 58.48 kJ/mol (13.98 kcal/mol). within the tolerance of 5%.

The induction period is reduced when the temperature of system increases because ,in effect ,the consumption of the impurities acting as inhibitor by free radicals increases.

The results in Figs. 4.18 and 4.19 show the gel effect phenomena in the same fashion described in Section 4.4.2. One contrast is that the gel effect occured earlier, at the almost early of polymerization which could be seen from Figs 4.18 and 4.19 at the studied temperatures above 70°C. The higher energy increases the reaction rate significantly and leads to the rapidly occurrence of gel effect resulting in the rapidly high limiting conversion.

However, the limiting conversion is dominated by both of the hybrid mechanism and the gel effect. The latter is more critical because the gel effect involves the autoaccelerated polymerization rate yielding high conversion. However, the limiting conversion never reach 100% conversion because the glass effect usually occurs after the gel effect (Section 2.3.3).
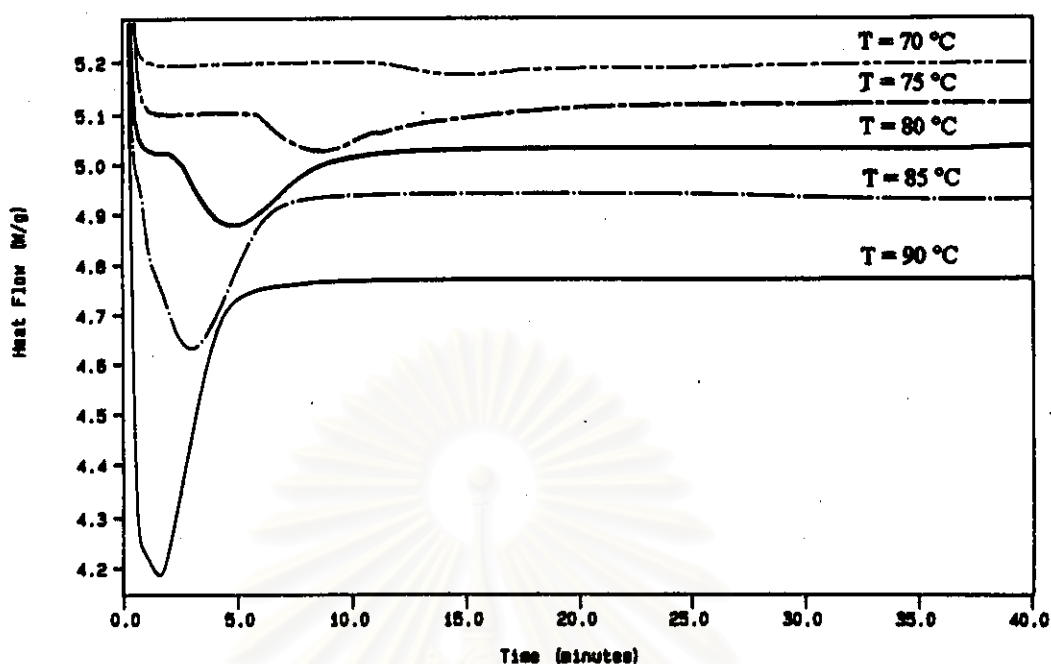
Fig. 4.18 DSC thermograms of the isothermal foamed polymerization of acrylamide ; [AM] = 2.44 mol/L . [K₂S₂O₈] = 1.22 x 10⁻³ mol/L , the polymerization temperatures are indicated on the curves .

TABLE 4.7

Heat of Polymerization and Limiting Acrylamide Conversion in

the Foamed Polymerization of Acrylamide with Variation

of Polymerization Temperature

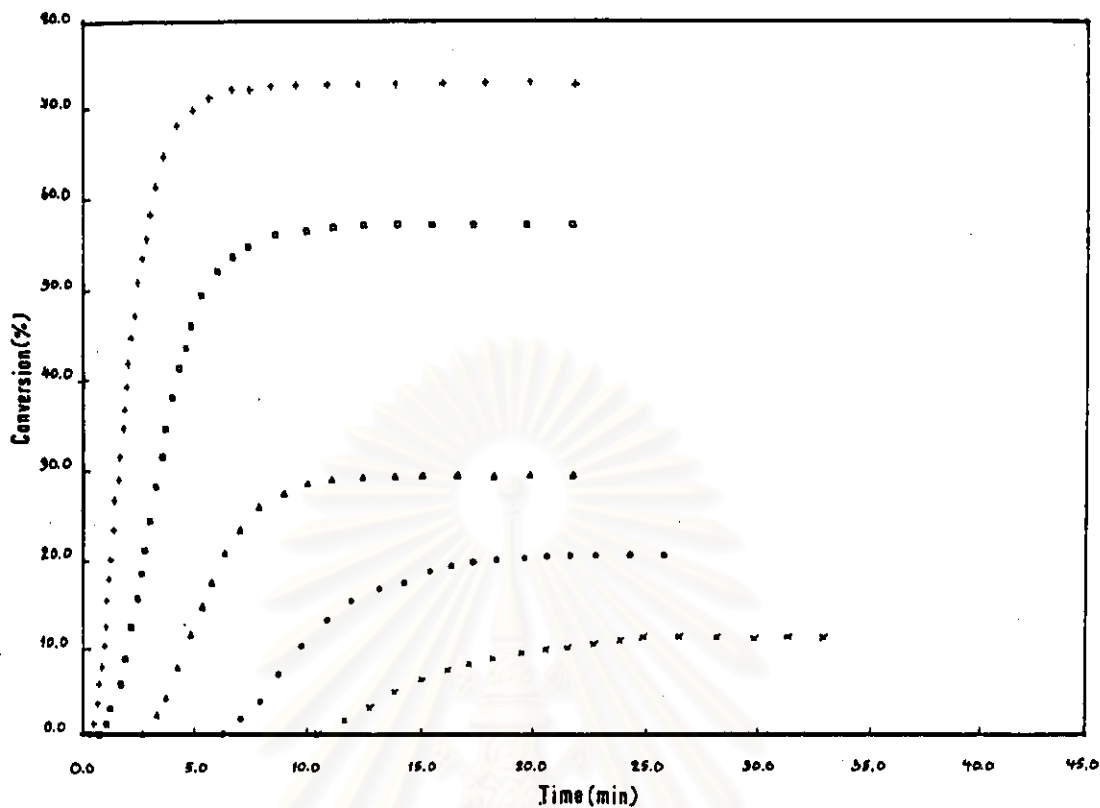| T (°k)	ΔH_S (J/g)	ΔH_I (J/g)	Limiting conversion (%)
343	129.600	14.056	10.85
348	129.600	26.044	20.10
353	129.600	37.676	29.07
358	129.600	73.938	57.05
363	129.600	94.120	72.62

Fig. 4.19 The plot of percentage of monomer conversion versus time of acrylamide polymerization in the foamed system ; [AM] = 2.44 mol/L , $[K_2S_2O_3]$ =1.22 x 10^{-3} mol/L with variation of T : (X) 70 , (O) 75, ($\triangle$) 80, ($\square$) 85, (+) 90°C .
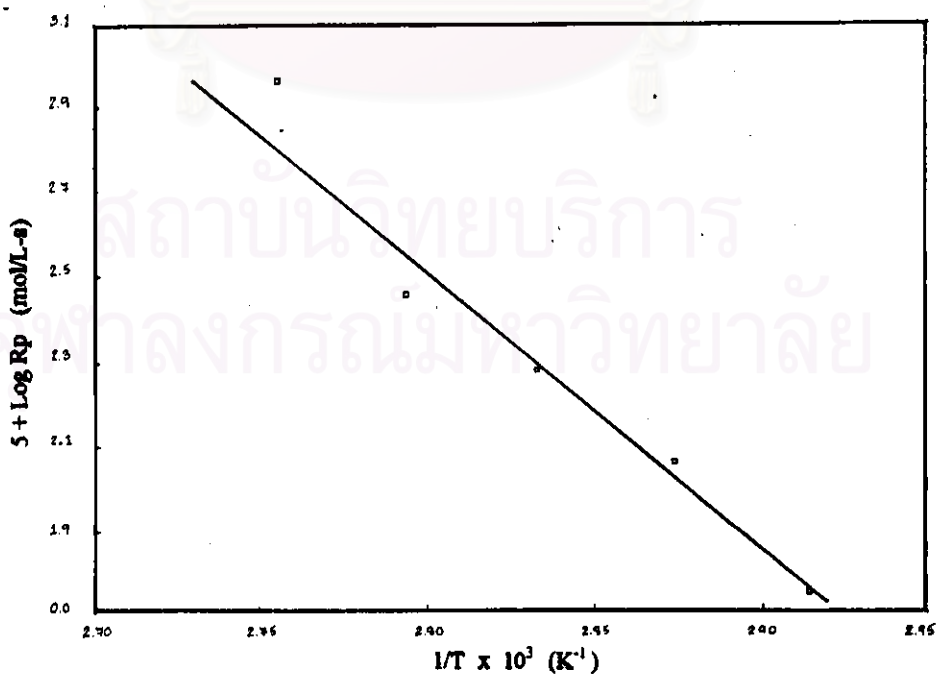

Fig. 4.20 The Arrhenius plot of log R_p vs. 1/T (K) for acrylamide polymerization in the foamed system ; [AM] = 2.44 mol/L, $[K_2S_2O_3]$ = 1.22 x 10^{-3} mol/L .

4.5 The Thermal Effects for Foamed Polymerization of Acrylamide

Indeed, the synthesis of polymers by the foamed polymerization technique takes place in the non-isothermal system during the course of polymerization because the temperature of system is allowed to rise exothermically, which is needed to create the autoacceleration reaction at the early stage of the polymerization (Section 2.2).

The effect of the polymerization temperature on the initial polymerization rate and percentage of conversion under the isothermal condition has been discussed in Section 4.4.3. When the polymerization temperature increases the initial polymerization rate and the percentage of monomer conversion increases. The higher polymerization temperature leads to the increase in occurrence of the gel effect and the limiting monomer conversion. Therefore, in the non-isothermal foamed system, the rate of polymerization and the percentage of monomer conversion is likely varied with the polymerization temperature of the system. This affects to the kinetics of polymerization reaction critically. The kinetics of this polymerization is more sophisticated.

Temperature of the non-isothermal foamed system which varies with the heat of exothermic polymerization may depend on many factors, including the reaction mass, scale for the polymer synthesis, the heat-transfering system (surface area/volume ratio of reactor, the number

and size of gas bubbles, the agitation system) and others. Some of these variables affecting to the initial rate of polymerization and percent conversion were studied.

The temperature profile and conversion profile of the non-isothermal foamed polymerization of acrylamide were determined according to experimental Sections 3.5.1 and 3.5.2. The results are shown in Figs.4.21 and 4.22.
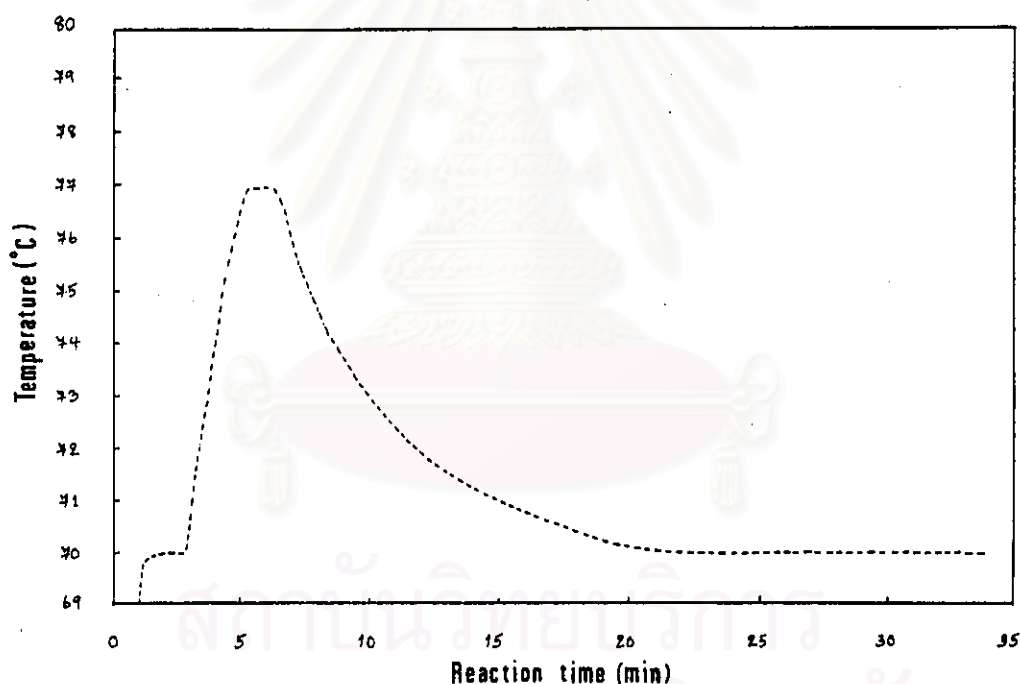

Fig. 4.21 Temperature profile for the non-isothermal foamed polymerization of acrylamide : $[K_2S_2O_8]$ = 1.22 x 10^{-3} mol/L , [AM] = 2.44 mol/L. Reaction conditions : ampoule diameter, 1 cm o.d. ; water bath temperatures, 70°C; scale for the synthesis, 5 cm.[3]

The maximum temperature difference (T_m-T_b) was found to be 7°C ; T_m is the maximum temperature of foamed system and T_b is the water bath temperature. The initial rate of polymerization and limiting conversion were found to be 9.45 x 10^{-3} mol/L-s and 69.73%,
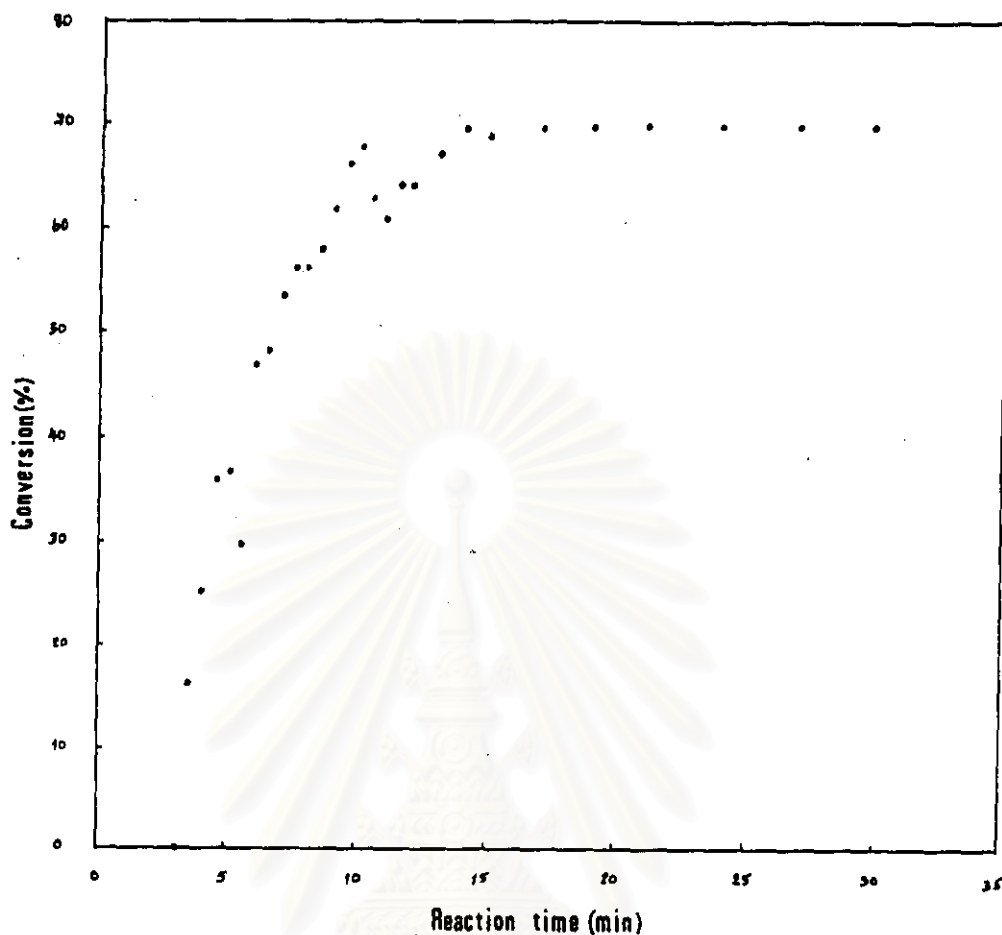
Fig. 4.22 Conversion profile for the non-isothermal foamed polymerization of acrylamide ; $[K_2S_2O_8]$ = 1.22 x 10^{-3} mol/L , [AM] = 2.44 mol/L. Reaction conditions : ampoule diameter, 1 cm. o.d.; water bath temperatures, $70^{\circ}C$; scale for the synthesis, 5 cm.^{3}

respectively. Compared with the data obtained in the case of the isothermal foamed polymerization of acrylamide in Section 4.4, the initial polymerization rate and limiting conversion in the non-isothermal foamed system become significantly higher.

The induction period was also found. When the temperature of the foamed system reached to the initial polymerization temperature the polymer mass could be formed after the induction period. However, the induction period was shorter than that of the isothermal foamed system

discussed in Section 4.4. It is clear that the temperature increment of the system during the course of polymerization leads to the occurrence of autoacceleration reaction earlier in the polymerization, which subsequencely affects to the initial rate of polymerization, the limiting conversion and the induction period significantly as mentioned above. The effects of this reaction are similar to the gel effect but more significant because it involves the autoacceleration reaction under the isothermal condition. The temperature or the thermal energy is the main factor determining the rate constants of elementary reactions of polymerization reaction (initiation, propagation, termination). The more the temperature increases, the higher the value of rate constants are. Therefore the rate constants of elementary reactions under the non-isothermal condition are likely higher than those under the isothermal condition.

In addition, the physical state of the foamed system enhances the autoacceleration reaction by increasing the chain radical lifetime. The isolation of bubbles and gel-like particles in the foamed system during the polymerization expands the growing chain radical life time. The temperature increment of the non-isothermal foamed system leads to the production of CO_2 gas bubbles from acid-base reaction in the foamed system and also bubbles from the evaporation of water. They help isolate gel-like particles further so as to the radical lifetime , which enhance the autoacceleration reaction.

4.6 The Effects of Reaction Scale, Surface Area/Volume Ratio of Ampoules and Reaction Mass on Temperature Profile and Conversion Profile.

When the reaction scale ,i.e.,an ampoule acting as a reactor or an increment of the reaction mass , increased the maximum temperature difference (T_m-T_b), the limiting conversion and the initial rate of polymerization of acrylamide in the non-isothermal system increased (Table 4.8, Fig 4.23, Fig. 4.24 and Fig. 4.25).

The reaction scale for the polymer synthesis correlates to the heat of polymerization. In larger scale the heat of polymerization is higher. The higher heat of polymerization needs to be eliminated and it is achieved in a better heat transfer design system. If the heat transfer system is not good enough, the accumulation of the heat in the system during polymerization occurs and leads to the promotion of auto-acceleration reaction. Then the rates of polymerization and conversion increase. Therefore, in the scaling up the synthesis of polymer in the non-isothermal foamed system, one should be concerned with this effect which affects to the control of the reaction ,i.e., the kinetics of polymerization ,and to some extent production reproducibility as well as polymer properties are affected.

TABLE 4.8

Reaction Conditions, Limiting Acrylamide Conversions and Initial Rates of Polymerization of the Non-Isothermal Foamed Polymerization of Acrylamide.

Reaction Scale (cm^3)	Diameter of reactor (cm)	wt.% of solvent (%)	T_m-T_b (°C)	Limiting conversion (%)	Initial rate of polymerization (mol/L-$s \times 10^3$)
0.5	1.0	70.59	2.0	63.28	5.95
5.0	1.0	70.59	7.0	69.73	9.45
5.0	2.0	70.59	11.0	78.70	13.13
5.0	1.0	43.61	43.0	94.65	42.87

The diameter of ampoules relates to the surface area/volume ratio of the reactor directly. Surface area/volume ratio becomes lower on increasing the diameter of reactor, resulting in the more difficult heat transfer in the polymerization system which enhances the autoacceleration reaction. In the design of the scale up reactor for the non-isothermal system, the appropriate heat transfer should not be omitted.

The reaction mass associates with the concentration of total reactants in the system. From the results and discussion in Section 4.4, one has to know that the increase in concentrations of the essential reactants, i.e., monomer and initiator bring about the higher initial rate
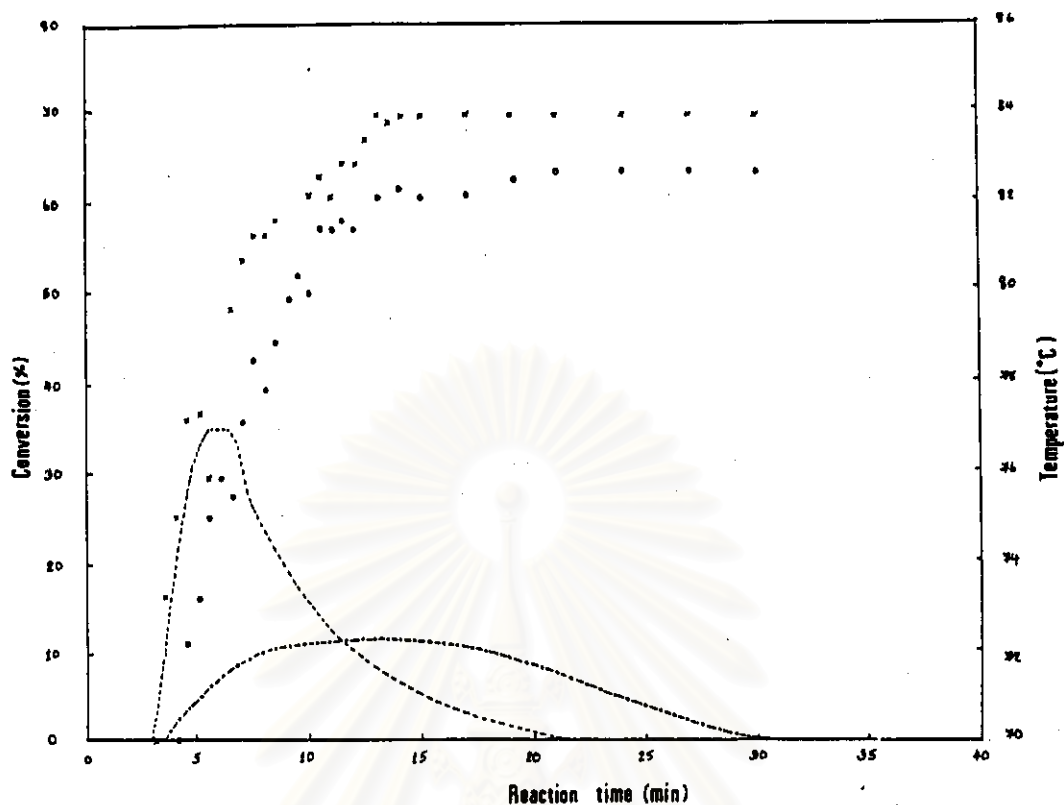
Fig. 4.23 Temperature (lines) and Conversion (symbols) profiles for the non-isothermal foamed polymerization of acrylamide ; $[K_2S_2O_8]$ = 1.22 x 10^{-3} mol/L , [AM] = 2.44 mol/L. Reaction conditions : ampoule diameter, 1 cm. o.d. ; water bath temperature, $70^{\circ}C$; scales for the synthesis are 0.5 (-•-) (O) , 5.0 (—) (X) cm^3

of polymerization and the monomer conversion , resulting in the higher heat of polymerization. The reaction mass is inversely proportional to the percentage of solvent (water). The more the reaction mass is, the lower the percentage of solvent appears. Therefore, in high reaction mass system, the polymer formed rapidly and simultaneously the very high viscosity is reached abrubtly because of the low amount of solvent. The very high rate and high viscosity lead to the difficulty of heat transter of system, thus , rising the temperature immediately. The autoacceleration takes place most seriously among the three effects (reaction scale , surface area/ volume ratio of reactor, reaction mass).
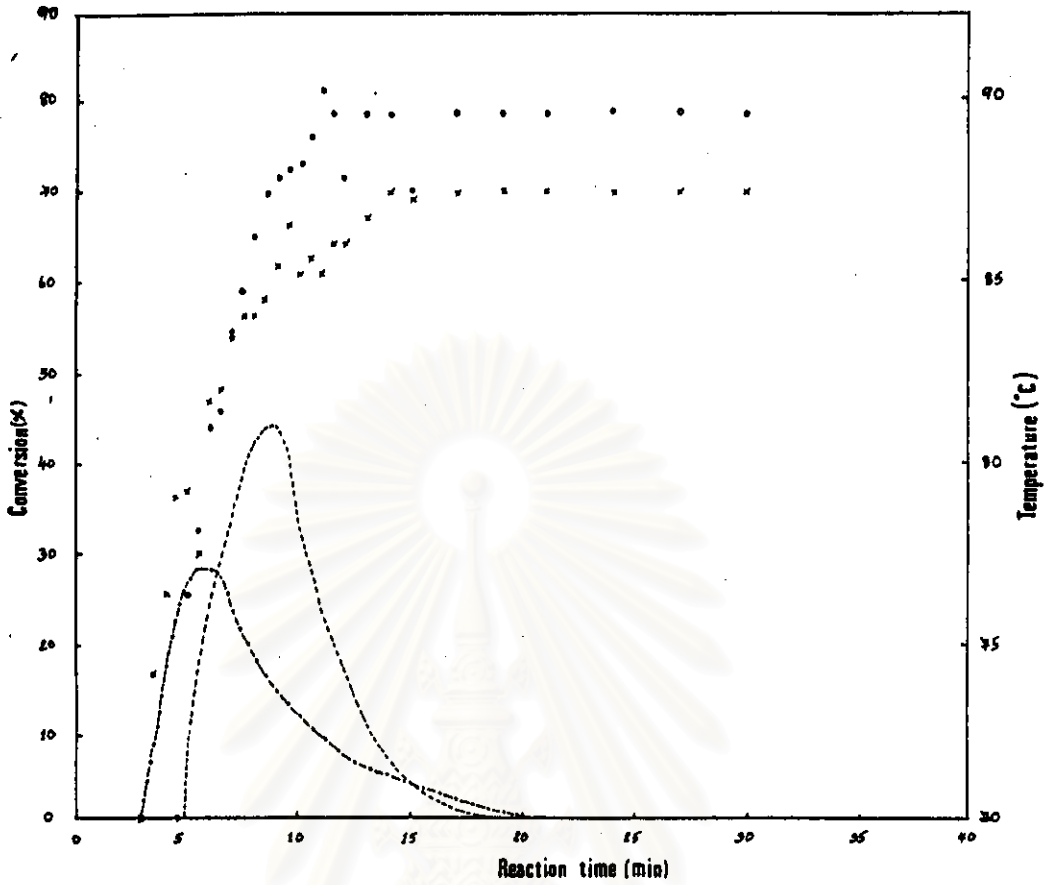
Fig. 4.24 Temperature (lines) and Conversion (symbols) profiles for the non-isothermal foamed polymerization of acrylamide ; [K$_2$S$_2$O$_8$] = 1.22x 10^{-3} mol/L , [AM] = 2.44 mol/L. Reaction conditions : ampoule diameters are 1.0 (--•--) (X) , 2.0 cm. (—) (O) o.d. ; water bath temperature, 70°C ; scales for the synthesis, 5.0cm.^{3} .

The very high initial rate of polymerization and limiting conversion can be reached within the very short period of the polymerization. However, the control of reaction and reproducibility is very difficult to made.

Also the rise in temperature in the non-isothermal foamed system studied above determines the numbers and sizes of gas bubbles which can be produced by the acid-base reaction and the evaporation of solvent (water). The bubbles enhance the autoacceleration reaction (Section 4.6). The different temperature rising value leads to the different
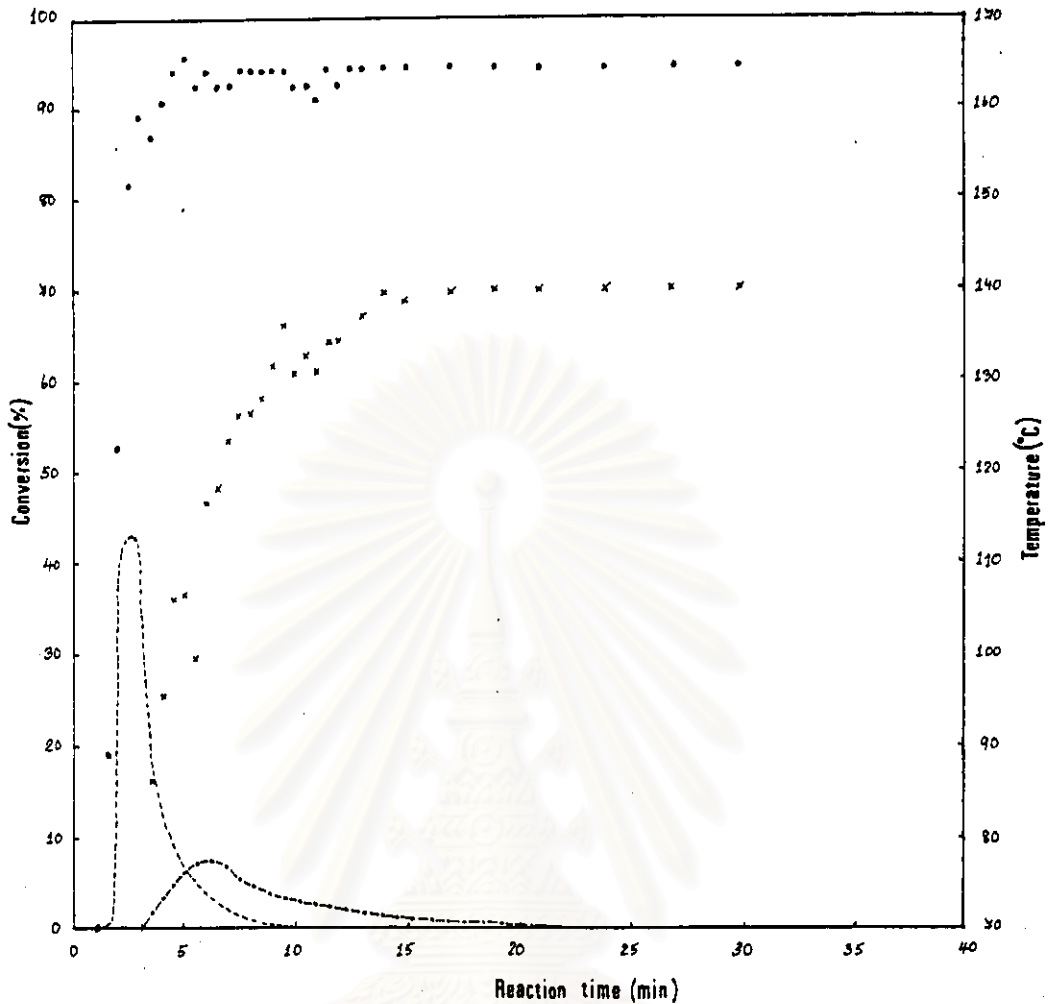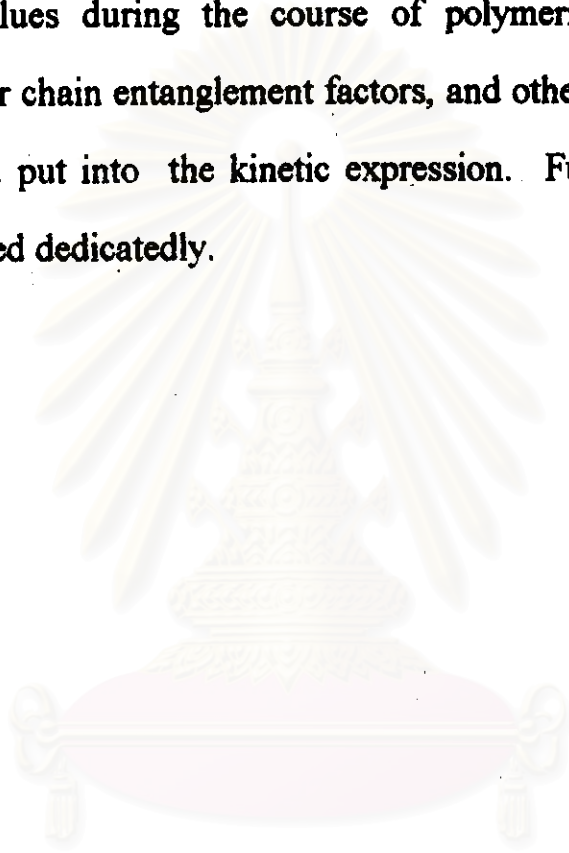
Fig. 4.25 Temperature (lines) and Conversion (symbols) profiles for the non-isothermal foamed polymerization of acrylamide at the different wt% of solvent (water) of 70.59% (—•—) (X), 43.61% (– –) (O). Reaction Conditions : ampoule diameters, 1 cm o.d. ; water bath temperature, 70°C ; scales for the synthesis, 5.0 cm³ ([AM] and [K₂S₂O₈] are varied with weight percent of solvent) .

numbers and sizes of gas bubbles which enhance autoacceleration reaction in different ways. These gas bubbles act as heat transfer agent simultaneously. Thus, the efficiency of heat transfer system also depends on the numbers and sizes of these gas bubbles. Finally, the gas bubbles take part in the control of the rise in temperature in the non-isothermal system.

The autoacceleration reaction in the non-isothermal foamed

system mentioned above is very complicated. Similarly, the kinetics of autoacceleration reaction in the non-isothermal foamed system are more sophisticated because of more kinetic determining factors such as the temperature values during the course of polymerization, the bubble system, polymer chain entanglement factors, and others which have to be determined and put into the kinetic expression. Further work on this aspect is required dedicatedly.